



Regular Research Manuscript

Extraction and Characterization of Fibres from the Bark of Ficus Nekbudu Tree

Liberato V. Haule

Department of Mechanical and Industrial Engineering, College of Engineering and Technology,
University of Dar es Salaam, P.O. Box 35131, Dar es Salaam Tanzania
liberato.haule@udsm.ac.tz; liberatohaule@yahoo.co.uk
ORCID: <https://orcid.org/0000-0001-7137-3267>

ABSTRACT

This paper investigates the extraction and characterization of fibres from the bark of the ficus nekbudu tree. The Ficus Nekbudu Fibres (FNF) was extracted from the bark by retting in water and then treatment with sodium hydroxide solution. The extracted FNF was analysed for chemical composition, physical, tensile, surface, structural and thermal stability properties. Findings on the chemical composition indicated that FNF has cellulose (49.9%), lignin (13.4%), ash (7.1%) and water content (8.1%). From the physical investigation it was found that FNF has density ($1.42 \pm 0.005 \text{ g/cm}^3$) and moisture regain ($9.2 \pm 0.3\%$). From mechanical investigation it was found that FNF has tenacity ($2.56 \pm 0.75 \text{ cN/dtex}$) and extension at break ($9.23 \pm 2.85\%$). SEM analysis indicated that FNF has rough surface with some surface impurities. The ATR- FTIR analysis indicates that the FNF has Total Crystallinity Index (TCI) and Lateral Order Index (LOI) of 0.52 and 0.41, respectively. Thermal analysis indicates that the FNF are stable up to 250°C.

ARTICLE INFO

Submitted: **June 3, 2023**

Revised: **Aug. 29, 2023**

Accepted: **Sep. 15, 2023**

Published: **Oct., 2023**

Keywords: *Ficus nekbudu, natural fibres, cellulose, extraction.*

INTRODUCTION

The rapid change in science, technology and innovation has expanded the use of textile fibres to include conventional (clothing) and non-conventional applications such as geotechnical, sports and medical (Lepot et al., 2023; McCarthy, 2016). Diverse use of textile fibres has led in increased demand, which can be addressed by more production of natural and synthetic fibres. Synthetic fibres dominate the market due to the availability of the raw material, relative low cost of production, easy modification to suit different applications or fashion needs and less impurities with consistent properties.

However, synthetic fibres pose some sustainability challenges in its life cycle (Kozłowski & Mackiewicz-Talarczyk, 2020). One avenue to mitigate the sustainability challenges of the synthetic fibres is to research more on natural fibres (Khan et al., 2022). The natural fibres can be animal, mineral or plant based. Plant based sources dominate the natural fibres' market. The plant based natural fibres are extracted from fruit, bark, stem or leaf of the plant. The extraction of the plant fibres involves breaking down the non-fibrous components, separating the fibres from the plant and processing the fibres into the required properties. The most common type of plant fibre is cotton while others include

sisal, flax, hemp, jute and kapok. Ficus nekbudu is a plant of moracea family grown in tropical countries including Tanzania, see Figure 1.



Figure 1: Ficus Nekbudu plant.

Traditionally, ficus nekbudu plant uses include animal feeds, traditional medicines and making of ropes. In addition, the ficus nekbudu fibres are used as absorbent for waste treatment (Prodromou & Pashalidis, 2016). The ropes made from the bark of ficus nekbudu tree are very strong hence are used for construction and agricultural activities. This suggests that, the bark contain strong fibrous materials.

The research on extraction and characterisation of fibres from the aerial roots of ficus tree has been reported by Ramesh and Rameshkannan (2021). The extracted cellulosic fibres were characterised for plastic reinforced composite. The fibres extracted from aerial roots of ficus tree have about 52% cellulose and thermally stable up to 200°C. Research has indicated that alkaline treatment of the fibres improved cellulose content, tensile strength and thermal stability (Rameshkannan & Ramesh Babu, 2022). The extracted fibres are used as a raw material for production of microcrystalline cellulose (Mugaanire et al., 2019). Extracting the fibres from the roots require complete uprooting of the tree, which encourages deforestation. The bark of the ficus nekbudu tree can potentially be used for extraction of fibres. The use of bark of

the tree does not require complete uprooting of the tree for making the fibres, hence minimal impact on the environment. However, literature suggests that there are no reported studies on extraction and characterization of the fibres from the bark of the ficus plant for textiles application. This paper reports on the extraction and characterization of fibres from the ficus nekbudu plant. The ficus nekbudu fibre (FNF) was characterized for cellulose composition, mechanical properties, thermal stability and water absorption properties.

MATERIAL AND METHODS

Material: The ficus nekbudu bark was obtained from Mbinga district in southern Tanzania. The bark was peeled from the stem of the ficus nekbudu tree and then packed in a plastic bag for transportation to laboratory for further processes. Analytical grade chemicals used such as sodium hydroxide (NaOH), acetic acid (CH₃COOH), sulphuric acid, dichloromethane, ethanol, sodium sulphite, sulphuric acid, hydrogen peroxide and xylene were purchased from Sigma Aldrich.

Equipment: Microbalance (Mettler Toledo density balance) with accuracy of $\pm 0.0001 \text{ g/cm}^3$

Extraction of the Fibres

The outer layer and inner layers of the bark was manually separated by peeling (Figure 2). Then, the inner layer was soaked in water for seven days for softening through rotting away some cellular tissues surrounding the fibres. The softened inner bark was manually separated into smaller fibre bundles followed by further treatment in NaOH solution (20%) at 30°C for 24 hours to remove non-cellulosic materials. The fibres were hot washed at 40°C for 10

minutes, cold rinsed. then air dried for one 24 hours.

The dry fibres (5 g) were placed in a solution containing H₂O₂ (16%) and NaOH (5% w/v) at 55°C, under continuous

agitation for 90 minutes. After cooling to room temperature, the fibres were filtered then washed with distilled water. The fibres were neutralized with CH₃COOH (0.1%) followed by cold rinsing and air dried.



Figure 2: Layers of the ficus nekbudu bark (Left Side-Outer layer, Right Side-Inner layer).

Characterisation of the Extracted Fibres

Determination of the Chemical Composition of the Fibres

The FNF was analysed for cellulose and lignin content using the method proposed in the literature (Vinod et al., 2021). A known weight of fibres was cut into small pieces and then crushed in a motor and paste to reduce the size. The crushed sample was divided into two portions of known weight. The first portion of the crushed fibres was treated in a solution of dichloromethane and later in 95% nitric acid in order to remove lignin, hemicellulose and other

non-cellulosic material. In order to get impurity free cellulose insoluble fraction, the fibres were washed in ethanol. The insoluble fraction was dried and then weighted for estimating the cellulose content.

The second portion of the sample was charged in a vessel with 75% sulphuric acid at 1:10 ratio of sample to acid for 30 minutes at 30°C to hydrolyse the non-lignin matters. The mixture was cooled and filtered on a sintered glass crucible to claim the acid insoluble lignin residue. The acid insoluble lignin was washed with water and oven dried for estimating the lignin content. The cellulose and lignin contents of FNF was estimated by calculating the weight of the dried residue samples expressed as

percentage of the original individual samples. The water and ash contents of FNF was determined as per the previously reported method (Vinod et al., 2021).

Determination of Density of the Fibres

The density of FNF was determined by using Toledo balance as per the previously reported approach (Haule et al., 2016b; Khan et al., 2022). FNF was first weighed in air and then weighed in the xylene (Liquid B) with density 0.865 g/cm^3 at 20°C . The weight of the fibres in air (A) and in liquid (B) and the temperature of the immersion liquid were recorded. The density of the immersion liquid at the recorded temperature was determined using Equation (1),

$$\rho_1 = \frac{\rho_0}{(\beta(T_f - 20) + 1)} \quad (1)$$

where: ρ_1 and ρ_0 are the densities of the xylene liquid during the test and at 20°C , respectively; β is the volumetric temperature coefficient of xylene liquid ($0.00086 \text{ v/v } ^\circ\text{C}$); T_f is the temperature of the xylene liquid during sample testing and The density of the fibres (ρ) was calculated using Equation (2).

$$\rho = \frac{A}{(A-B)[(\rho_1 - \rho_2) + \rho_2]} \quad (2)$$

The ρ_2 is density of air (0.001165 g/cm^3). Five replicates were measured and the average recorded.

Tensile Properties of the Fibres

The tensile properties of FNF was determined by using Instron, Series IX Automated Materials running by Bluehill 3 version 3.41 software. The tested specimens were pre-conditioned at 65% relative humidity and 23°C for 24 hours prior to the test. The testing was carried out in a room conditioned at 61% relative humidity and 25.3°C . The test method was in accordance to the British standards (BS EN ISO 1924-2:2008) (British Standards, 2008). During testing, a pre-tensioning of 10 kN and crosshead speed of 2 mm/min

were applied to the fibres. The samples were clamped in the Instron jaws as per the previously reported approach (Haule et al., 2016b). The reported mean data includes tensile strength and elongation at break.

Thermal Stability of the Fibres

The thermal stability of FNF was determined by using an STA PT-1000 thermo gravimetric analyser (TGA). The equipment was calibrated by heating 5 mg of dry fibres loaded in alumina crucibles at a heating rate of 10°C/min up to 600°C under an oxygen atmosphere as previously reported (Teng et al., 2018).

Scanning Electron Microscopic Analysis

The surface morphology of FNF was investigated using a Hitachi EDAX-S300N SEM instrument. The fibres were pre-gold coated using a SEM E5100 system (Polaron Limited) which was operated at 0.01 torr with current of 20.0 mA for three minutes. For all SEM imaging the secondary electron (SE) detector and a 5 kV accelerating voltage was used.

ATR-FTIR Analysis of the Fibres

The ATR-FTIR spectra were collected on Nicolet 5700 with diamond crystal. Scanning was performed from 4000 to 600 cm^{-1} with 128 repetitions and a resolution of 8 cm^{-1} . The ATR-FTIR crystallinity indices of FNF was determined in accordance to the previously proposed method (Haule, Carr, and Rigout, 2016a; Nelson and O'Connor, 1964a, 1964b). Previously the Total Crystallinity Index (TCI) and the Lateral Order Index (LOI) of cellulosic fibres was estimated as the ratios of the FTIR $1372/2900 \text{ cm}^{-1}$ and $1420/893 \text{ cm}^{-1}$ peak intensities, respectively. In this work the TCI and LOI of FNF were estimated as ratios of $1370/2899 \text{ cm}^{-1}$ and $1420/898 \text{ cm}^{-1}$ intensities, respectively. The ATR-FTIR data were processed using Origin Pro 8.1 SR3 application software.

Determination of the Moisture Regain

The moisture regain of FNF was determined gravimetrically with the fibres conditioned at 20°C and relative humidity of 65% for 24 hours prior to testing. Conditioned samples weighing 50 mg were contained in a pre-dried sample holders and then dried in an oven at 110°C for 2 hours. The samples were immediately transferred into a desiccator containing phosphorus pentoxide to allow cooling. After cooling, the samples were then weighed immediately to avoid moisture resorption. Finally, the moisture regain was calculated as the amount of moisture in the sample expressed as a percentage of its dry weight. Five replicates were done and the average result were calculated.

RESULTS AND DISCUSSION

Physical Properties and Chemical Composition of the Fibres

Determination of the physical properties of FNF involved the analysis of appearance, length, density and moisture regain, Table 1. FNF is curled in bundles with average length of 32 cm. However, the fibres could be easily disentangled manually into individual fibres, which made it easy to conduct a single fibre tensile test. This suggests that the fibres extraction process may be coupled with a combing system to ensure separation into individual fibres. FNF is yellowish in colour, which is similar to linen fibres.

Table 1: Physical properties of FNF

S/N	Properties	Value
1	Color	Yellowish
2	Length	32±0.5 cm
3	Density	1.42±0.005 g/cm ³
4	Moisture regain	9.2±0.3 %

Findings indicate that the density of FNF is 1.42 ±0.005 g/cm³, Table 1. The density of the fibres is within the range of the density of other natural fibres, which ranges from 1.1 g/cm³ to 1.5 g/cm³ (Vinod *et al.*, 2021). The higher density may limit light applications of the fibres in weight textile applications.

Examination of the moisture uptake properties, indicates that moisture regain of FNF was 9.2 ±0.3%, Table 1. This moisture regain suggests that the FNF may deliver comfort similar to other natural cellulosic fibres such as cotton, linen and flax.

Examination of the chemical composition of FNF, indicates that the cellulose, lignin, ash, wax and water contents are within other plant fibres content, Table 2. The chemical composition indicates that FNF

has cellulose content of 49.9%, which is less by 2.7% compared to fibres extracted from the aerial roots of ficus tree (Ramesh Babu and Rameshkannan, 2021). Comparison of cellulose content with other natural fibres from bark or plants shows that the cellulose content of FNF is 11.6% higher than vachellia farnesiana fibres (Vijay *et al.*, 2020), 22.5% lower than dichrostachys cinerea fibres (Baskaran, Kathiresan, SenthamaraiKannan, and Saravanakumar, 2018) and 6.56% lower than acacia nilotica L. plant fibres (Kumar *et al.*, 2022). The cellulose content of FNF was lower than the fibres extracted from other parts of plants as indicated in Table 2. The higher the cellulose content, the higher the fibre strength and thermal stability.

Table 2: Chemical composition of FNF

S/N	Fibre source	Cellulose (wt. %)	Lignin (wt. %)	Ash (wt. %)	WC (wt. %)	Reference
1	Bark of ficus nekbudu	49.9	13.4	7.1	8.1	Current study
2	Stem of cardiospermum halicababum	59.82	9.3	4.5	1.9	(Vinod et al., 2021)
3	Saccharum bengalense grass (Sarkanda)	53.45	11.7	5.6	2.1	(Vijay et al., 2020)
4	Phaseolus vulgaris	62.17	9.13	9.02	6.1	(Gurukarthik et al., 2019)
5	Heteropogon contortus plant	64.87	13.56	-	7.4	(Hyness et al., 2018)
6	Bark of dichrostachys cinerea	72.4	16.89	3.97	9.82	Baskaran et al., 2018
7	Barks of vachellia farnesiana	38.3	9.1	6.21	11	(Vijay et al., 2020)
8	Stem of momordica charantia	61.2	4.8	2.24	6.3	(Khan et al., 2022)
9	Bark of acacia nilotica L. plant	56.46	8.33	4.95	-	(Kumar et al., 2022)
10	Rhectophyllum camerunens	68.2	15.6	-	-	(Béakou et al., 2008)

The lignin content of FNF was 13.4%, which is lower than the fibres extracted from bark of dichrostachys cinerea (Baskaran et al., 2018) but higher than the rest of the bark fibres as indicated in Table 2. The high lignin content may be responsible for the fibre bundle formation. The FNF ash and moisture contents are 7.1% and 8.1%, respectively.

Mechanical Properties of FNF

Findings on the mechanical properties indicate the tenacity of FNF as 2.56 ± 0.75 cN/dtex, which is above the tenacity of sarkanda fibres (Vijay et al., 2020). However, the tenacity of fibres may vary due to methods of extraction, type of plant and chemical composition. Examination of Table 3 indicates that FNF elongation at break was $9.23 \pm 2.85\%$. This average elongation value implies that the FNF may easily be formed into fabrics with draping properties similar to other natural fibres such as cotton.

Table 3: Mechanical properties of FNF

Property/Variation	Load at Tensile strength [N]	Elongation at break [%]	Tenacity [cN/dtex]
Mean	30.59	9.23	2.56
Standard deviation	8.95	2.85	0.75
Coefficient of variation	29.25	30.89	29.25

Surface Analysis of Fibres

Examination of the surface morphology indicates that FNF has rough textural features

with some surface impurities, Figure 3. This suggests a need for optimization of the extraction process to ensure fibres with high

purity and minimum surface damage. The presence of surface impurities is not uncommon feature as it has been previously reported in the literature (Vijay *et al.*, 2020). The surface impurities could be due to the extraction method or handling of the fibres during characterization. A feature to the extracted fibres is that, unlike other similar fibres, FNF has minimal surface cracks.

FTIR Analysis of FNF

Examination of the FTIR spectra indicates that the broad band in $3600\text{-}3000\text{ cm}^{-1}$ was assigned to hydrogen bonds between OH groups of cellulose structure, while the 3328 cm^{-1} intensity was due to the OH stretching for intermolecular hydrogen bonds in the

cellulose. Previous research indicated that the broad band is for the cellulose II-unit cell while other research reported the band at 3334 cm^{-1} as due to O-H stretching of cellulose and hemicellulose (Kumar *et al.*, 2022). The band at 2899 cm^{-1} is assigned to the CH stretching in less ordered alkyl chain and impurities such as wax and allied hydrocarbons structures (Baskaran *et al.*, 2018; Carrillo *et al.*, 2004; Nelson & O'Connor, 1964a; Široký *et al.*, 2010). The band at 1623 cm^{-1} is assigned to the OH water absorbed in the cellulose. However, the literature suggests that the OH water absorbed in the cellulose is detected by the band at 1635 cm^{-1} (Hyness *et al.*, 2018; Široký *et al.*, 2010) and the reasons for such variations could be due to differences in nature and extraction methods of the cellulose.

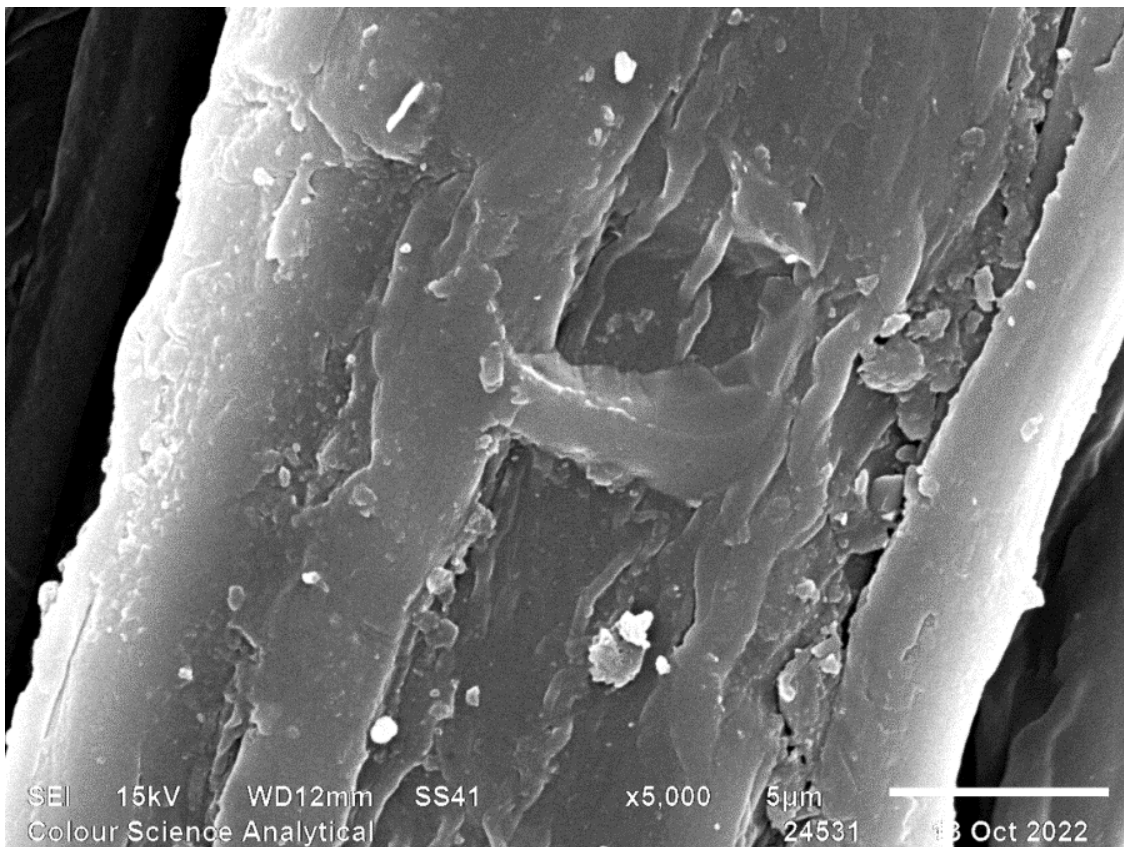


Figure 3: SEM micrograph of ficus fibres at 5000 x magnification at 15 kV.

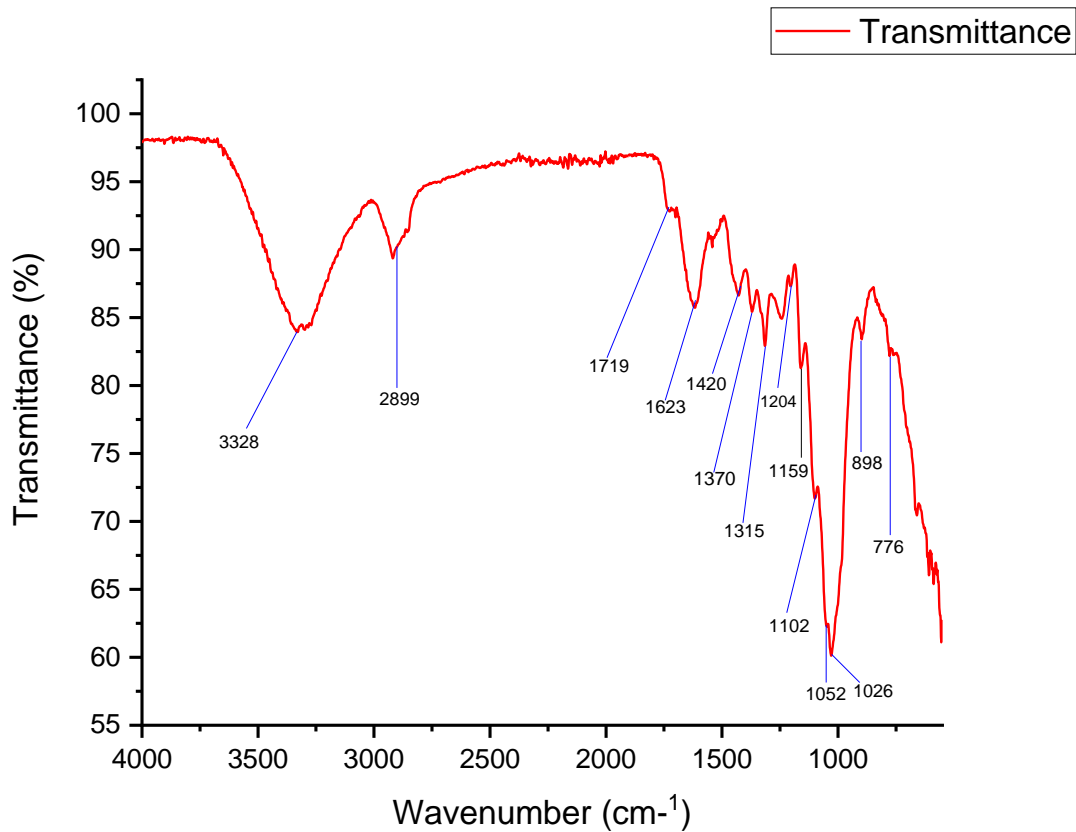


Figure 4: FTIR Spectrum for the Ficus Nekbudu fibres in the 400 cm^{-1} to 500 cm^{-1} wave number.

The absorption bands at 1370 cm^{-1} and 1315 cm^{-1} were assigned to CH bending, OH in-plane bending and CH₂ wagging of the cellulose structure (Baskaran et al., 2018; Carrillo et al., 2004; Colom & Carrillo, 2002; Kumar et al., 2022; Nelson & O'Connor, 1964a, 1964b; Široký et al., 2010). The band at 1204 cm^{-1} was assigned to the OH in-plane bending in cellulose structure (Carrillo et al., 2004; Široký et al., 2010). The 1159 cm^{-1} and 1102 cm^{-1} bands were assigned to C-O-C asymmetric stretching from the β -glycosidic bond in cellulose and the ring asymmetric valence in cellulose respectively (Vinod et al.,

2021). The 1052 cm^{-1} and 1026 cm^{-1} bands were due to the C-OH stretching and aromatic ring due to bending and vibration of C-H and C-O respectively (Hyness et al., 2018) (Vijay et al., 2020). The 898 cm^{-1} band was assigned to the C-O-C valence vibration of the β -glycosidic link or deformation at C (1) in cellulose II structure (Carrillo et al., 2004; Colom & Carrillo, 2002; Nelson & O'Connor, 1964a, 1964b; Široký et al., 2010). To conclude, FNF has demonstrated a mixture of cellulose I and cellulose II forms with the characteristics absorption bands summarized in Table 4.

Table 4: FTIR bands for FNF

Frequency (cm^{-1})	Vibrational Assignments	References
3334	O-H stretching of cellulose and hemicellulose	(Hyness et al., 2018; Kumar et al., 2022)
2899	C-H stretching, less ordered alkyl chain due to impurities such as wax and allied hydrocarbons	(Baskaran et al., 2018; Carrillo et al., 2004; Nelson & O'Connor, 1964a; Široký et al., 2010)

Frequency (cm ⁻¹)	Vibrational Assignments	References
1685-1655	C=O stretching	(Široký et al., 2010)
1635	OH of water absorbed from cellulose	(Carrillo et al., 2004; Hyness et al., 2018; Široký et al., 2010)
1420	CH ₂ scissoring at C(6)	(Carrillo et al., 2004; Colom & Carrillo, 2002; Nelson & O'Connor, 1964a, 1964b; Široký et al., 2010)
1370	CH bending	(Carrillo et al., 2004; Colom & Carrillo, 2002; Nelson & O'Connor, 1964a, 1964b; Široký et al., 2010)
1315	CH ₂ wagging	(Baskaran et al., 2018; Carrillo et al., 2004; Colom & Carrillo, 2002; Kumar et al., 2022; Nelson & O'Connor, 1964a, 1964b; Široký et al., 2010)
1204	OH in plane bending	(Carrillo et al., 2004; Široký et al., 2010)
1159	C-O stretching due to lignin	(Vinod et al., 2021)
1101	C-O stretching	(Vinod et al., 2021)
1052	C-OH stretching due to lignin	(Hyness et al., 2018; Vijay et al., 2022)
1028	C-OH stretching due to lignin	(Khan et al., 2022; Vinod et al., 2021)
1024	Aromatic ring due to bending and vibration of C-H and C-O respectively	(Vijay et al., 2020)
898	C-O-C valence vibration	(Carrillo et al., 2004; Colom & Carrillo, 2002; Nelson & O'Connor, 1964a, 1964b; Široký et al., 2010; Vinod et al., 2021)

Total Crystallinity Index and Lateral Order Index of the Fibres

Findings on the peak intensities ratio of 1370.9/2899 cm⁻¹ indicates that the total crystallinity index (TCI) for FNF was 0.52. Similarly, the peak intensities ratio of the 1420/898.8 cm⁻¹ indicates that the lateral order index (LOI) for the fibres was 0.41. The TCI and LOI values are less than viscose and lyocel fibres (Carrillo et al., 2004). The low TCI indicates that the amount of crystalline regions in FNF is low and less ordered hence low strength. Similarly, the low LOI indicates that the degree of alignment of the polymer chains is less for FNF than lyocel and viscose fibres.

Fibre Thermal Stability

Findings on the thermal stability indicates that FNF weight loss was identified into five regions marked as A, B, C, D and E, Figure 5.

In the region A, the rate of change of fibre weight with temperature was very fast, which is probably due to traces of non-cellulosic unstable impurities in the fibres. These impurities seem to be volatile at a temperature below 100 °C. Region B (100 °C to 250 °C), is characterized by low rate of change of weight. The features in the second region may be due to structural changes of FNF due to release of structurally bound water and low molecular weight substances. Region C (250 °C to 350 °C), is characterised by very high rate of change of fibre weight with temperature. At this stage the fibres' structure is highly degraded due to the high temperature applied into the material. This degradation continues but at slower rate up to about 450 °C, region D. Region E is characterized by a constant rate of mass loss with temperature, which indicates that the fibre structure is completely destructed due to the effects of heating. This thermal gravimetric profile suggests that FNF can withstand processing and finishing temperature of cellulosic fibres such as dyeing and curing of functional

finishes. The highest curing temperature of cellulosic fibres is about 180 °C for not more than 5minutes.

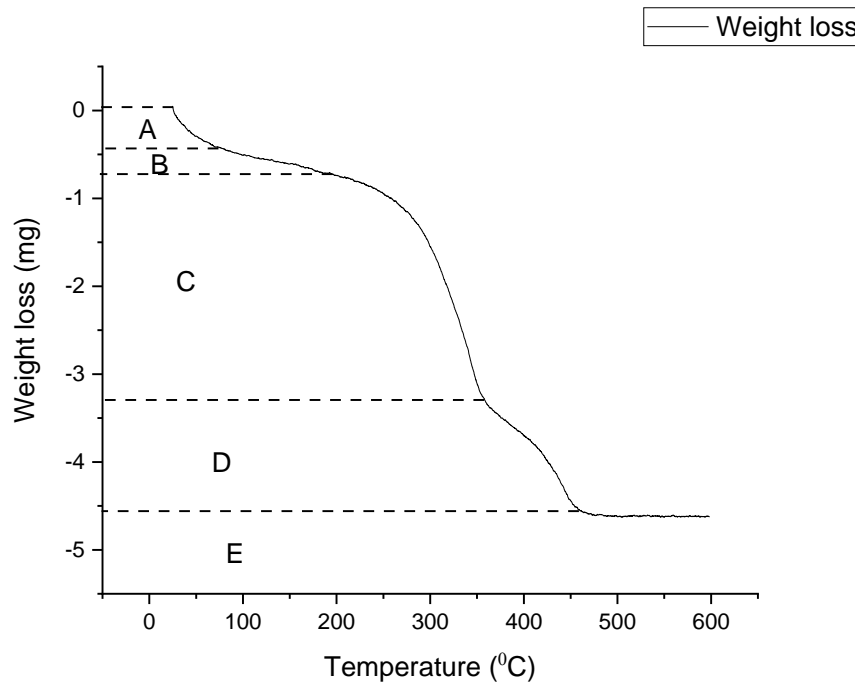


Figure 5: TGA curve for the ficus nekbudu fibres.

CONCLUSION AND RECOMMENDATION

FNF was successfully extracted from the bark of the ficus nekbudu tree by water retting followed by sodium hydroxide treatment. Characterization of the selected properties of the fibres indicates that the density, moisture regain, tensile and surface properties are similar to other natural cellulosic fibres. ATR-FTIR analysis indicates that the fibres are made up of cellulose I and cellulose II forms. Thermal analysis findings have indicated that the fibres are stable to textile finishing temperatures. Further study is recommended to optimise extraction process, determines detailed chemical composition and perform dyeability tests of the fibres.

REFERENCES

- Baskaran, P.G., Kathiresan, M., Senthamaraiannan, P., & Saravanakumar, S.S. (2018). Characterization of New Natural Cellulosic Fiber from the Bark of *Dichrostachys Cinerea*. *Journal of Natural Fibers*, **15**(1): 62-68. <https://doi.org/10.1080/15440478.2017.1304314>.
- Béakou, A., Ntenga, R., Lepetit, J., Ateba, J.A., & Ayina, L.O. (2007). Physico-chemical and microstructural characterization of “*Rhctophyllum camerunense*” plant fiber. *Composites Part A: Applied Science and Manufacturing*, **39**(1): p. 67-74. <https://doi.org/10.1016/j.compositesa.2007.09.002>.
- Beentje, H.J., & Mbago, Frank M. (2007). A Guide to the Fig Trees of Western Tanzania with Special Emphasis on Gombe and Mahale National Parks. *Journal of East African Natural History*, **96**(1): 1-26.
- British Standards. (2008). Paper and board. Determination of Tensile Properties. Constant Rate of Elongation Method (20 mm/min): BS EN ISO 1924-2:2008. Retrieved 11 January 2012, from British Standards Online

- <https://bsol.bsigroup.com/en/Bsol-Item-Detail-Page/?pid=000000000030164688>
- Carrillo, F., Colom, X., Sunol, J.J., & Saurina, J. (2004). Structural FTIR Analysis and Thermal Characterisation of Lyocell and Viscose-type Fibres. *European Polymer Journal*, **40**(9): 2229-2234. <https://doi.org/10.1016/j.eurpolymj.2004.05.003>.
- Colom, X., & Carrillo, F. (2002). Crystallinity Changes in lyocell and Viscose-type Fibres by Caustic Treatment. *European Polymer Journal*, **38**(11): 2225-2230. [https://doi.org/10.1016/S0014-3057\(02\)00132-5](https://doi.org/10.1016/S0014-3057(02)00132-5).
- Gurukarthik Babu, B., Prince Winston, D., SenthamaraiKannan, P., Saravanakumar, S.S., & Sanjay, M.R. (2019). Study on characterization and physicochemical properties of new natural fiber from Phaseolus vulgaris. *Journal of Natural Fibers*, **16**(7): 1035-1042. <https://doi.org/10.1080/15440478.2018.1448318>.
- Haule, L.V., Carr, C.M., & Rigout, M. (2016a). Investigation into the supramolecular properties of fibres regenerated from cotton based waste garments. *Carbohydrate Polymers*, **144**: 131-139. <https://doi.org/10.1016/j.carbpol.2016.02.054>.
- Haule, L.V., Carr, C.M., & Rigout, M. (2016b). Preparation and physical properties of regenerated cellulose fibres from cotton waste garments. *Journal of Cleaner Production*, **112**: 4445-4451. <https://doi.org/10.1016/j.jclepro.2015.08.086>.
- Hyness, N.R.J., Vignesh, N.J., SenthamaraiKannan, P., Saravanakumar, S.S., & Sanjay, M.R. (2018). Characterization of New Natural Cellulosic Fiber from Heteropogon Contortus Plant. *Journal of Natural Fibers*, **15**(1): 146-153. <https://doi.org/10.1080/15440478.2017.1321516>.
- Khan, A., Raghunathan, V., Singaravelu, D.L., Sanjay, M.R., Siengchin, S., Jawaid, M., Alamry, K.A., & Asiri, A.M. (2022). Extraction and Characterization of Cellulose Fibers from the Stem of Momordica Charantia. *Journal of Natural Fibers*, **19**(6): 2232-2242. <https://doi.org/10.1080/15440478.2020.1807442>.
- Kozłowski, R.M., & Mackiewicz-Talarczyk, M. (2020). 1A - Introduction to natural textile fibres. In Kozłowski, R.M. & Mackiewicz-Talarczyk, M. (Eds.), *Handbook of Natural Fibres (Second Edition)* (pp. 1-13): Woodhead Publishing.
- Kumar, R., Sivaganesan, S., SenthamaraiKannan, P., Saravanakumar, S.S., Khan, A., Ajith Arul Daniel, S., & Loganathan, L. (2022). Characterization of New Cellulosic Fiber from the Bark of Acacia nilotica L. Plant. *Journal of Natural Fibers*, **19**(1): 199-208. <https://doi.org/10.1080/15440478.2020.1738305>.
- Lepot, L., Vanhouche, M., Vanden, D.T., & Lunstroot, K. (2023). Interpol review of fibres and textiles 2019-2022. *Forensic Science International: Synergy*, **6**: 100307. <https://doi.org/10.1016/j.fsisyn.2022.100307>.
- McCarthy, B.J. (2016). An overview of the technical textiles sector. *Handbook of Technical Textiles*, 1-20.
- Mugaanire, I.T., Wang, H., & Sun, J. (2019). Fibrous microcrystalline cellulose from Ficus natalensis barkcloth. *European Journal of Wood and Wood Products*, **77**(3): 483-486. <https://doi.org/10.1007/s00107-019-01382-2>.
- Nelson, M.L., & O'Connor, R.T. (1964a). Relation of Certain Infrared Bands to Cellulose Crystallinity and Crystal Lattice Type. Part II. A New Infrared Ratio for Estimation of Crystallinity in Celluloses I and II. *Journal of Applied Polymer Science*, **8**(3): 1325-1341.

- <https://doi.org/10.1002/app.1964.070080323>.
- Nelson, M.L., & O'Connor, R.T. (1964b). Relation of Certain Infrared Bands to Cellulose Crystallinity and Crystal Latticed Type. Part I. Spectra of Lattice Types I, II, III and of Amorphous Cellulose. *Journal of Applied Polymer Science*, **8**(3): 1311-1324.
<https://doi.org/10.1002/app.1964.070080322>.
- Prodromou, M., & Pashalidis, I. (2016). Europium adsorption by non-treated and chemically modified opuntia ficus indica cactus fibres in aqueous solutions. *Desalination and Water Treatment*, **57**(11): 5079-5088.
<https://doi.org/10.1080/19443994.2014.1002431>.
- Ramesh, B.S., & Rameshkannan, G. (2021). Aerial Root Fibres of Ficus amplissima as a Possible Reinforcement in Fibre-Reinforced Plastics for Lightweight Applications: Physicochemical, Thermal, Crystallographic, and Surface Morphological Behaviours. *Journal of Natural Fibers*, 1-16.
<https://doi.org/10.1080/15440478.2021.1958422>.
- Rameshkannan, G., & Ramesh Babu, S. (2022). Effect of Alkalization on Physical, Chemical, Morphological and Mechanical Properties of Aerial Root Ficus Amplissima Fibre. *Journal of Natural Fibers*, 1-15.
<https://doi.org/10.1080/15440478.2022.2051671>.
- Široký, J., Blackburn, R., Bechtold, T., Taylor, J., & White, P. (2010). Attenuated Total Reflectance Fourier-transform Infrared Spectroscopy Analysis of Crystallinity Changes in Lyocell Following Continuous Treatment with Sodium Hydroxide. *Cellulose*, **17**(1): 103-115.
<https://doi.org/10.1007/s10570-009-9378-x>.
- Teng, Y., Yu, G., Fu, Y., & Yin, C. (2018). The preparation and study of regenerated cellulose fibers by cellulose carbamate pathway. *International Journal of Biological Macromolecules*, **107**, 383-392.
<https://doi.org/10.1016/j.ijbiomac.2017.09.006>.
- Vijay, R., James, D.J.D., Gowtham, S., Harikrishnan, S., Chandru, B., Amarnath, M., & Khan, A. (2022). Characterization of Natural Cellulose Fiber from the Barks of Vachellia farnesiana. *Journal of Natural Fibers*, **19**(4): 1343-1352.
<https://doi.org/10.1080/15440478.2020.1764457>.
- Vijay, R., Singaravelu, D.L., Vinod, A., Paul Raj, I.D., Franklin, S.M.R., & Siengchin, S. (2020). Characterization of Novel Natural Fiber from Saccharum Bengalense Grass (Sarkanda). *Journal of Natural Fibers*, **17**(12): 1739-1747.
<https://doi.org/10.1080/15440478.2019.1598914>.
- Vinod, A., Vijay, R., Singaravelu, D.L., Sanjay, M.R., Siengchin, S., Yagnaraj, Y., & Khan, S. (2021). Extraction and Characterization of Natural Fiber from Stem of Cardiospermum Halicababum. *Journal of Natural Fibers*, **18**(6): 898-908.
<https://doi.org/10.1080/15440478.2019.1669514>.